ULTRASONIC IMAGING 5, 331-345 (1983)

IMPROVEMENTS IN THE SPECTRAL DIFFERENCE METHOD FOR MEASURING ULTRASONIC ATTENUATION

Michael Insana, James Zagzebski, and Ernest Madsen

Medical Physics Department
University of Wisconsin
1300 University Avenue
Madison, WI 53706

The accuracy of the spectral difference method for measuring ultrasonic attenuation has been investigated using tissue-mimicking phantoms. Attenuation coefficients of the phantom materials were measured using a narrow-band substitution technique and compared with the results of the spectral difference method. Agreement within ±10 percent was typical for measurements in homogeneous materials. The best agreement between the spectral difference and substitution techniques was obtained when effects due to transducer beam diffraction were taken into account in the analysis. This was found for two types of homogeneous tissue-mimicking materials, both having speed of sound and attenuation properties similar to human liver but each with different backscatter properties. The effects of inhomogeneous tissues interposed between the transducer and the interrogated volume were also studied by simulating these conditions in phantoms. Experimental techniques which minimize the effects of perturbations introduced by these inhomogeneities are suggested.

Key words: Attenuation; diffraction; phantoms; spectrum; ultrasound.

I. INTRODUCTION

A number of techniques have been proposed for measuring the ultrasonic attenuation properties of soft tissues, *in vivo* [1-7]. An important consideration in such measurements is the dependence of the attenuation coefficient (α) on frequency (f). The model $\alpha = \alpha_o f^n$ has been used to describe this dependence, where α_o is a constant of proportionality and n is the frequency dependence (typically ~ 1 for many soft tissues [8]). In general, these attenuation parameters are estimated from the changes in the spectrum of a broadband pulse as it propagates through tissue.

In early *in vitro* measurements, Kuc [1,3] estimated α_o for liver by comparing the spectrum of a broadband pulse reflected from a planar interface, with and without a volume of liver interposed. Assuming the interrogated pulse had a Gaussian shaped spectrum and that attenuation of liver tissue was proportional to frequency (n=1), a downward shift in the peak frequency of the attenuated spectrum was used to estimate α_o. This method of estimating the attenuation has been termed the spectral shift method. The spectral shift method was later applied to *in vivo* measurements by Flax, et al., [7] using a zero crossing method and by Dines and Kak [6] in their work in ultrasonic attenuation tomography.

0161-7346/83 $3.00

Kuc also proposed a "spectral difference" method for measuring α_o [2,3]. Here attenuation is estimated using acoustic pulses that can have a spectrum of arbitrary shape. In this method, power spectra are calculated for segments of backscattered echo signals originating from different depths in the tissues. The ratio of discrete spectral values at two tissue depths may be used to calculate α_o and the frequency dependence, n. Both broadband [2,5] and narrow-band [4] pulses have been used in similar techniques to make attenuation estimates, in vivo.

An important aspect of these measurements is the presence of spectral variations with tissue depth that are independent of attenuation. For example, transducer beam diffraction and focusing effects will produce such variations. Although these effects have been noted previously [4,9,19,20], their magnitudes have not been thoroughly investigated. In this investigation, the influence of such effects on the spectral difference method of measuring ultrasonic attenuation has been studied using tissue-mimicking (TM) phantoms. Since the attenuation properties of the phantom materials were known, it was possible to determine the accuracy of attenuation estimates using the spectral difference method. It was also possible to demonstrate the magnitude of errors introduced by beam diffraction and focusing properties of the transducer and to determine correction factors to reduce this source of error.

Homogeneous phantoms represent an "ideal" medium for studying tissue characterization techniques. In clinical practice, however, the situation may be more complicated because of additional artifacts introduced by the transmission path between the transducer and the region of interest (for example, see figure 5) or because of inhomogeneities in the medium itself. In the present investigation, we have studied the consequences of measuring α_o for TM phantoms in which beam distorting fat-nonfat surfaces were simulated. In some circumstances, large errors in α_o measurements were introduced by such layers. Experimental conditions for which these perturbing effects were minimized are reported.

II. A METHOD OF ACCOUNTING FOR DIFFRACTION EFFECTS

In this section, a brief summary of the spectral difference method described by Kuc [1,3] is presented. A simple modification to this technique which includes the effects of the transducer beam diffraction pattern is then described.

A broadband acoustic pulse is transmitted into an attenuating medium by placing the transducer onto the medium surface (Fig. 1a). A portion of the transmitted acoustic energy is scattered back to the transducer by the medium, producing an r.f. signal as shown in figure 1b. A segment of this waveform is time gated and the power spectrum of the segment calculated. A mean power spectrum is then determined for r.f. waveform segments recorded from adjacent, but spatially uncorrelated tissue volumes. These volumes are all centered an axial distance r from the transducer surface. The plane perpendicular to the beam axis at the measurement distance r is often refered to as a C-plane. The mean power spectrum, S(r,f), is calculated from the individual spectra, using

$$S(r,f) = \frac{1}{M} \sum_{i=1}^{M} |s_i(r,f)|^2 \quad , \tag{1}$$

where $s_i(r,f)$ represents the ith Fourier transform of a single time gated r.f. waveform and M is the number of waveforms recorded at depth r.

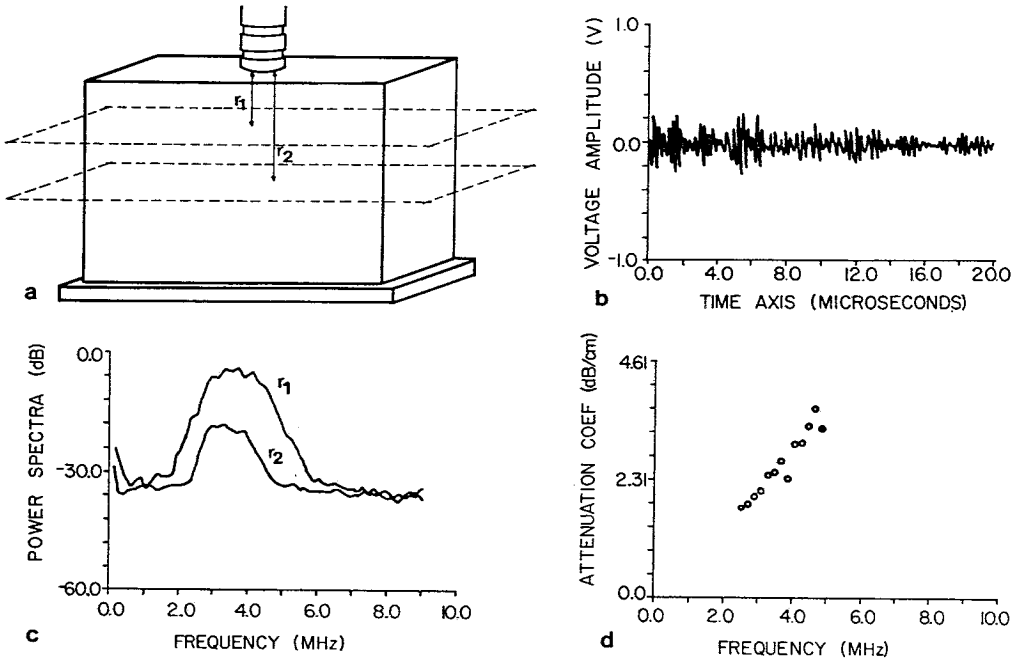

Fig. 1 An illustration of the spectral difference method for measuring attenuation using a tissue mimicking (TM) phantom (α_o = 0.7 dB cm-1 MHz-1). A transducer is scanned laterally across the phantom surface (a). At each lateral position, an r.f. waveform is detected (b). Waveform segments, each corresponding to a phantom depth, r, are recorded and processed to give the mean power spectrum for that depth (c). These power spectra are then used to find the attenuation coefficients over the transducer bandwidth (d).

The mean power spectra from two depths, r_1 and r_2, in the medium (Fig. 1c) can be related using,

$$S(r_2,f) = H(r_1,r_2,f)\ S(r_1,f) \quad . \tag{2}$$

$H(r_1,r_2,f)$ is defined as the power transfer function which, in general, includes all processes contributing to transform the power spectrum measured at depth r_1 to that measured at r_2.

In Eq. (2), there exists the assumption that the ensemble of scattering particles distributed throughout the medium at depth r_2 have the same scattering properties as the material at depth r_1. That is, the scattering cross section and the frequency dependence of scattering at r_2 and r_1 are assumed to be equivalent.

If attenuation were the only transformation process and assuming that attenuation is proportional to frequency (n=1), then

$$H(r_1,r_2,f) = e^{-2\Delta r\, \alpha_o' f} \quad . \tag{3}$$

In Eq. (3), the proportionality constant, α_o', has the units [cm^{-1} MHz^{-1}] and $\Delta r = r_2 - r_1$.

Solving for the attenuation coefficient, α, in units of [dB/cm], yields

$$\alpha = \alpha_o f = \frac{5}{\Delta r} \log \frac{S(r_1,f)}{S(r_2,f)} \tag{4}$$

(Note: log refers to $\log_{10}$.) Refering to figure 5.1, Eq. (4) can be interpreted in the following manner. The attenuation coefficient at frequency, f, can be found from the logarithm of the mean power spectra calculated from echo signals obtained at C-plane depths r_2 and r_1 and from the distance between the two measurement planes Δr. Examples of attenuation coefficients calculated from the spectra in figure 1c are shown in figure 1d. The constant, α_o, is the slope of the attenuation coefficient versus frequency and can be calculated in the following manner:

$$\alpha_o = \frac{5}{N\Delta r} \sum_{i=1}^{N} \left[\log \frac{S(r_1,f_i)}{S(r_2,f_i)}\right] / f_i \quad . \tag{5}$$

N is the number of discrete frequency values averaged.

In practical situations, factors in addition to attenuation modify the echo signal spectrum as the depth of the scattering volume changes. Variations introduced by beam diffraction, producing, for example, the spectral changes noted in figure 2b, must be included in the transfer function $H(r_1,r_2,f)$. In this investigation, empirically derived correction factors were found which, when applied to the raw spectral data, improved the accuracy of measuring attenuation in homogeneous phantoms.

Correction factors were found for each transducer used by performing the experiment diagrammed in figure 2a. A cylindrical volume of a macroscopially-homogeneous tissue-mimicking material (i.e., no large-scale regions of varying ultrasonic properties) was placed in a water-alcohol

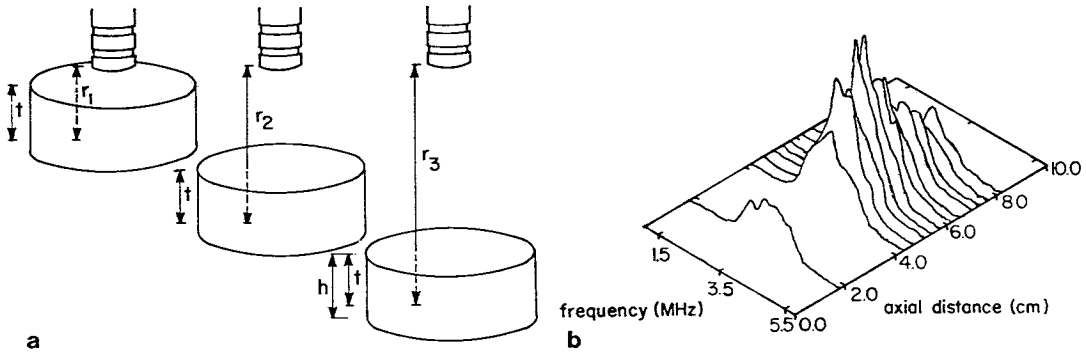

Fig. 2 A description of the experiment (a) and a sample of the resulting data (b) used to measure transducer beam correction factors, X(r,f), for application in the spectral difference method (Eq. (8)). Typical experimental values are h=2.5 cm, t=1.8 cm, and r ranging from 1.8 cm to 8.2 cm in steps of approximately 4 mm.

mixture. The TM sample had a large, planar surface that was oriented perpendicular to the beam axis. Beginning with the transducer on the sample surface, twenty-five r.f. echo signals were recorded from adjacent, nonoverlapping lines of sight. For each waveform, the power spectrum of a 5μs segment, originating from a volume centered 1.8 cm below the proximal surface, was calculated and an average of all the waveforms was found. This was repeated for a range of transducer-scattering volume distances extending to a depth of 8.2 cm, in steps of 4 mm. For each distance, r, the total amount of TM material between the transducer and the gated volume remained unchanged (1.8 cm). If the attenuation of the water-alcohol mixture is ignored, the only parameter which changes is the separation between the transducer and the scattering volume. Therefore, variations observed between the mean echo signal power spectra with increasing distance, r, (Fig. 2b) were attributed to transducer beam diffraction and focusing effects.

The spectral values measured in this experiment are called X(r,f). These functions represent the backscattered spectrum measured from a homogeneous TM material at different distances from the transducer, but without any change in attenuation. If we assume that transducer beam diffraction effects and ultrasonic attenuation contribute independently to the mean power spectrum, then these effects are separable. Therefore, estimates of attenuation can be obtained independent of the perturbing diffraction effects by dividing $X(r_i,f)$ spectral values into the corresponding mean power spectrum values, $S(r_i,f)$, to give

$$\frac{S(r_2,f)}{X(r_2,f)} = \frac{S(r_1,f)}{X(r_1,f)} \; e^{-2\Delta r \alpha_o' f} \quad . \tag{6}$$

Therefore, for homogeneous materials, the net transfer function in Eq. (2) becomes

$$H(r_1,r_2,f) = \frac{X(r_2,f)}{X(r_1,f)} \; e^{-2\Delta r \alpha_o' f} \quad . \tag{7}$$

α_o is then estimated using the expression:

$$\alpha_o = \frac{5}{N\Delta r} \sum_{i=1}^{N} \left[\log \frac{S(r_1,f_i)}{S(r_2,f_i)} - \log \frac{X(r_1,f_i)}{X(r_2,f_i)} \right] / f_i \quad . \tag{8}$$

Throughout this study, we have assumed that attenuation is proportional to frequency. This condition exists for the TM materials used in the present work [13] and has also been found for many soft tissues [8]. However, in general, this assumption is not necessary. That is, Eq. (8) could easily be adapted to include materials which are not proportional to frequency.

III. TESTING THE MODIFIED SPECTRAL DIFFERENCE METHOD

a) Tissue mimicking phantoms and materials

Experiments were performed to test the accuracy of the spectral difference method, both with and without the X(r,f) correction terms applied. Attenuation was measured for a range of depths in macro-

scopically-homogeneous tissue-mimicking materials. Since the attenuation properties of each phantom material were known, it was possible to determine the accuracy of this spectral difference method. During phantom construction, standard test cylinders (7.5 cm diameter, 2.5 cm thick) were produced from each "batch" of material made. The attenuation coefficients and the speeds of sound of the material in these test cylinders were measured using a narrow-band, substitution technique [12]. Results of these measurements are referred to as the expected or known attenuation properties of each phantom material and were used to compare with the spectral difference measurement results. Known attenuation and speed of sound values for each phantom component are given in table 1.

In a second set of experiments, the same measurements were made, but with a layer of TM fat material interposed between the transducer and the homogeneous TM material. The effects of inhomogeneous, overlying tissues on attenuation measurements could thus be observed.

Figure 3 shows diagrams of the phantoms used in this study. The TM fat material in phantoms I and II is an oil-in-gelatin dispersion having ultrasonic properties which mimic those of human fat [12]. It is composed of 50 percent water-based gelatin, 25 percent olive oil, and 25 percent kerosene, into which 0.065 g/cm^3 of microscopic, hollow glass spherical scatterers are added. The net density is 0.94 g/cm^3.

The material labelled TM nonfat A is a water-based gelatin containing a random distribution of microscopic graphite scattering particles [13]. A graphite powder concentration of 57.14 grams per liter gelatin was used, resulting in a net density of 1.06 g/cm^3. The speed of sound and attenuation of this material are similar to those of human liver. Also, Rayleigh scattering characteristics have been observed in the material [14].

The material in phantom III, labelled TM nonfat B, is described in [15]. The major components of this material are microscopic graphite particles mixed in molten agar. The agar suspension is formed into spheres of diameters ranging from 0.6 mm to 2.4 mm. The bulk phantom

Table 1

ACOUSTIC PROPERTY	PHANTOM I		PHANTOM II		PHANTOM III
	TM fat	TM nonfat A	TM fat	TM nonfat A	TM nonfat B
speed of sound (m/s)	1458	1570	1459	1567	1522
slope of the attenuation coefficient (dB/cm/MHz)	0.64	0.56	0.60	0.53	0.70

Speed of sound and attenuation properties measured for test cylinders of TM phantom materials. Results were obtained using a narrow-band substitution method. All measurements were made at 22°C, the speed of sound was measured at 2.0 MHz, and $\alpha_o = \alpha/f$ was averaged from 2.0 to 5.0 MHz.

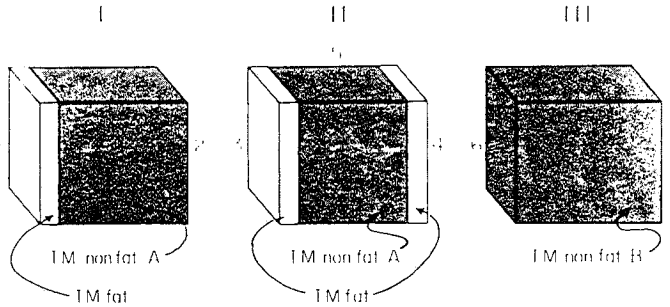

Fig. 3 Diagram of the three phantoms used in this study to test the spectral difference technique. Scanning surfaces 2, 5, and 6 provide direct access to the homogeneous, nonfat tissue mimicking materials. Beneath each of the scanning surfaces 1, 3, and 4, a different shape TM fat layer is interposed between the outside surface and the TM nonfat material.

material consists of these spheres closely packed in a solution of 5 percent n-propyl alcohol in distilled water. The average density of the composite material is 1.04 g/cm^3. Like TM nonfat A, TM nonfat B has attenuation and speed of sound properties similar to human liver. In addition, both Rayleigh scatterers, in the form of graphite particles, and intermediate size scatterers, represented by the agar spheres, are present. The relative contributions from these components are such that the ultrasonic backscatter coefficients of TM nonfat B are representative of backscatter coefficients in human liver tissue for the 1 to 7 MHz range [16].

The bulk of each phantom is encased in a Plexiglas box. Scanning surfaces 1 through 6 (Fig. 3) are covered with 160 micron thick Saran Wrap (Dow Chemical). The entire phantom is thus sealed from the atmosphere. All three phantoms provide a large, rectangularly shaped volume (16 cm x 14 cm x 5 cm) of ultrasonically-homogeneous TM nonfat material having known acoustic properties.

Scanning surfaces 2, 5, and 6 provide a direct acoustic window to the TM nonfat materials A and B. Measurements of α_o may be made through these surfaces without the perturbation of a TM fat layer. The overlying TM fat layers on surfaces 1, 3, and 4 are approximately 2 cm thick and are in intimate contact with the nonfat material. The boundary between the TM fat and nonfat materials of surface 4 is planar. The fat layers of surfaces 1 and 3 form an irregular (nonplanar) boundary with the nonfat material. These two surfaces differ somewhat in the nature of the surface irregularities.

The shape of the irregular boundaries is shown in figure 4. This figure shows phantom II at an intermediate step of its production, just prior to adding the fat layer. The mold used to produce this surface was made using a 1.25 inch diameter ball endmill to cut "randomly" into a Plexiglas surface. The Plexiglas was then used as a die to form a 1 mm thick polyethylene sheet from which the graphite-gelatin surfaces were cast. Following this, the polyethylene sheet was removed and the TM fat material poured into an overlying reservoir. While both irregular interfaces are similar in shape, one is inverted. That is, the hemispherical undulations which compose surface 3 stick up into the fat layer instead of down into the nonfat material as in surface 1.

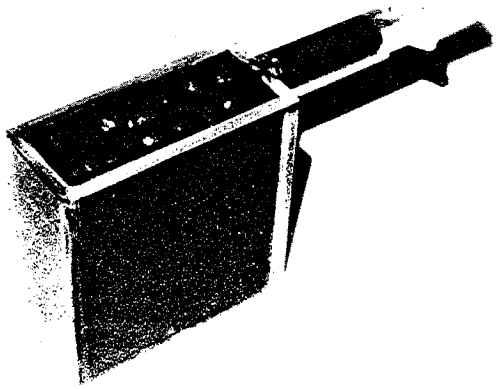

Fig. 4 Phantom II, just prior to adding a TM fat layer. This photograph shows the shape of the irregular TM fat-nonfat interface beneath scanning surface 3. The dimensions of the phantom are 16 cm x 14 cm x 5 cm. The diameter of the hemispherical irregularities is 1.25 inches.

The choice of irregular surface shape was a compromise between the dermis-subcutaneous fat interfaces observed while examining the abdominal wall tissue samples obtained during five autopsies. Skin samples were taken from the edges of the normal incision lines from lower to upper abdomen. The slices were to extend from the epidermis through to the underlying fascia. The bright yellow color of adipose tissue made it easily discernable from the white integument. Four of the samples presented a range from reasonably planar to gently undulating surfaces separating the dermis from the subcutaneous fat. The fifth sample, however, exhibited 1 mm to 5 mm fat globules imbedded throughout the dermis (Fig. 5). The effects of refraction and phase cancellation are expected to be extensive where there is the largest deviation from a planar fat-nonfat interface.

Fig. 5 Photograph of two sections of abdominal skin and subcutaneous tissue obtained during an autopsy of a 68-year-old male. The contrast seen between the darker subcutaneous fat regions and the white skin tissue has been enhanced. Both samples are 5 cm long.

b) Experimental instrumentation and methods

The apparatus assembled to measure α_o using the modified spectral difference method is shown in figure 6.

A pulser-receiver was used to excite a broadband transducer and linearly amplify the returning echo signals. The output signals were further amplified by a second receiver and then digitized with a Biomation Model 8100 transient recorder. An LSI 11/23 microprocessor controlled the transient recorder and the storage of digitized waveforms on a Winchester disk.

Twenty-five backscatter waveform segments, each 5 μs in duration, were acquired from a single phantom depth, r, by moving the transducer laterally across the scanning surface. The duration of the waveform segment was chosen to be short enough so that attenuation of acoustic energy within the gated region could be ignored. The power spectrum of each 500 point waveform segment (100 MHz sampling rate) recorded at r was calculated using an FFT algorithm and the results averaged to give a mean power spectrum, S(r,f). S(r,f) was measured at various phantom depths between 1.8 cm and 8.2 cm. These spectral measurements were then used to measure α_o using Eqs. (5) and (8).

A 3.5 MHz, 13 mm diameter Aerotech transducer, having a 4 cm to 8 cm focal region and a 3.5 MHz, 19 mm diameter Aerotech transducer, with a 6 cm to 13 cm focal region were used in this study. The -20 dB bandwidth was measured for each transducer using a plane reflector placed in a distilled-water bath. A broadband pulse reflected by the planar surface located within the transducer focal region was recorded and the frequency spectrum calculated. A center frequency of 3.5 MHz and a -20 dB bandwidth extending from 2.5 to 5.0 MHz was found for both transducers.

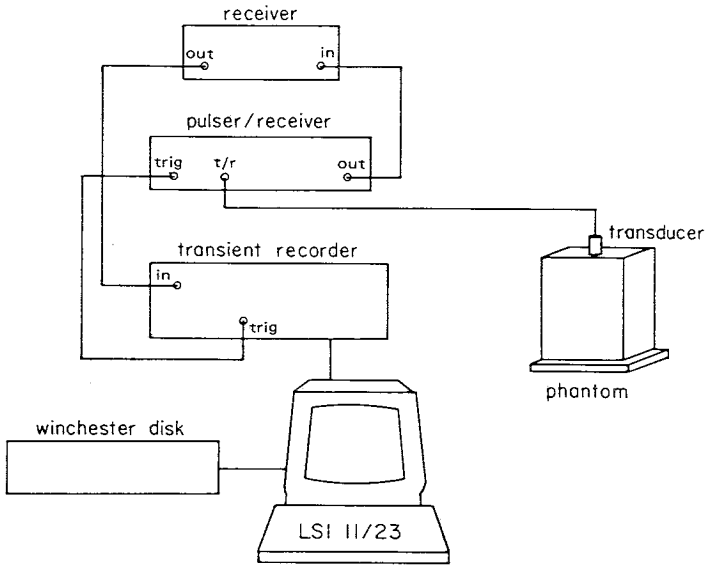

Fig. 6 Block diagram of apparatus for measuring attenuation using the spectral difference technique.

IV. RESULTS

An example of X(r,f) values measured for a 3.5 MHz/13 mm transducer having a focal length of approximately 6.0 cm is shown in figure 2b. The test cylinder sample contained TM nonfat material A. The mean amplitude spectrum from the gated echo signals are plotted over the focal region of the transducer, 4.0 cm to 8.0 cm. Notice that the spectral values vary significantly at different axial distances. For this transducer, the magnitude of the frequency components appears greatest near the focal length. Ultrasonic reverberations between the transducer and the sample surface obscured the data at distances between 1.8 cm and 4.2 cm.

Attenuation measurements for a homogeneous phantom, both with and without the X(r,f) spectrum corrections are shown in figure 7. In this and subsequent figures, a reference power spectrum was determined from a C-plane measurement at depth r_1. The data points represent values obtained by measuring the mean power spectrum at more distal C-plane depths in the phantom (r_2) and then using Eq. (5) or Eq. (8) to calculate α_o based on differences with the reference spectrum. Each data point represents an α_o value calculated for a different choice of second C-plane depth, r_2. Narrow-band substitution measurements on test cylinders of TM nonfat A for phantom I (see Table 1) yielded an α_o value of 0.56 dB cm^{-1} MHz^{-1}. This is indicated in the figures by the dashed line.

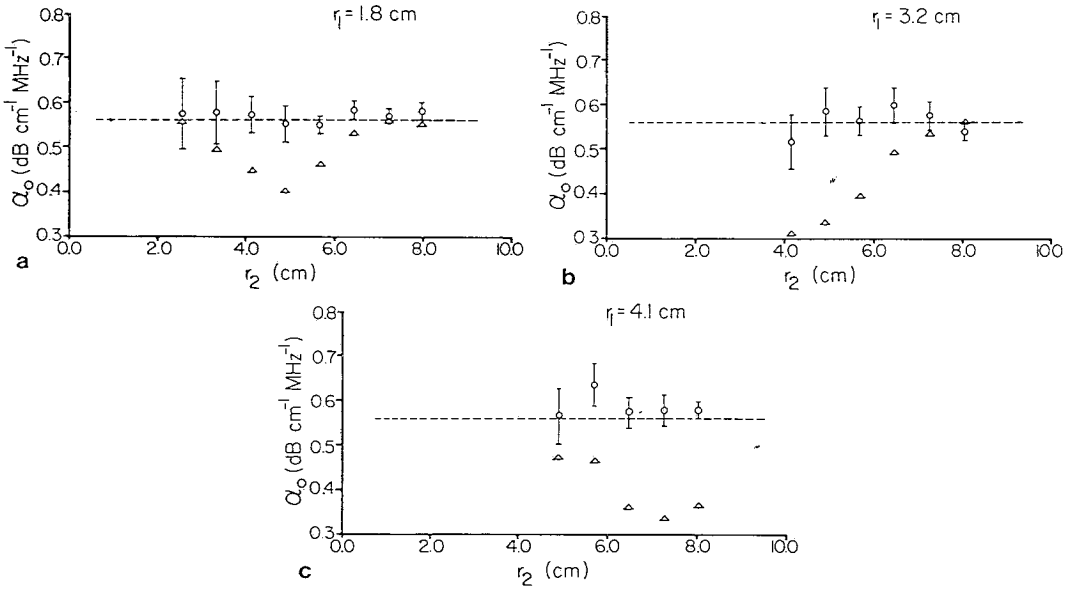

Fig. 7 Plots of the attenuation constant, α_o, for phantom I, scanning surface 2 (no intervening TM fat layer). Measurements of α_o with (o) and without (Δ) transducer beam correction factors, X(r,f), are compared with the known value (0.56 dB cm-1 MHz-1, dashed line). A 3.5 MHz/13 mm transducer was used in (a) and (b) and a 3.5 MHz/19 mm transducer was used in (c). Spectrum measurements are made at two phantom depths: r1 (proximal) and r2 (distal). The r1 value remained constant in each plot while r2 varied to demonstrate the influence of transducer beam diffraction effects on measurements of α_o. Error bars denote one standard deviation of the mean value.

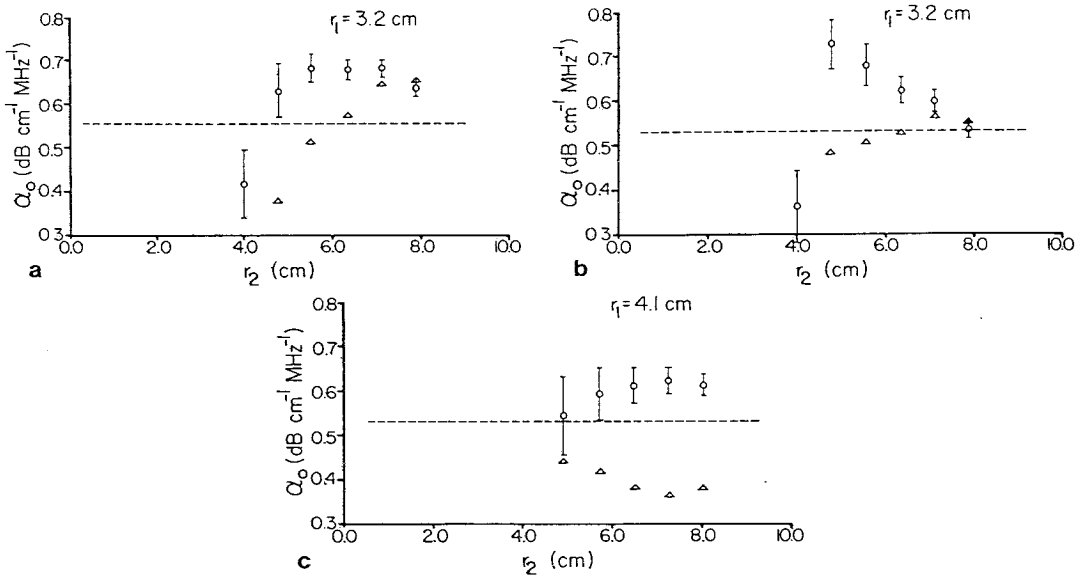

Fig. 8 Measurements of α_o from spectra obtained through irregular TM fat layers, with (o) and without (Δ) corrections for the transducer beam in the analysis. A 3.5 MHz/13 mm transducer was scanned across phantom I, surface 1 to obtain (a) and phantom II, surface 3 to obtain (b). In plot (c), α_o was measured using a 3.5 MHz/19 mm transducer, scanned across surface 3. The dashed lines mark the α_o value that was measured for test cylinders using a substitution method.

Attenuation measurements for phantoms I and II, but obtained through interposed TM fat layers, are shown in figures 8 and 9. Figure 8 shows the results of α_o measured through two different irregular TM fat-TM nonfat interfaces. In figure 9, a planar fat layer was interposed.

Finally, in figure 10, attenuation measurements as a function of depth in phantom III (TM nonfat B) are illustrated.

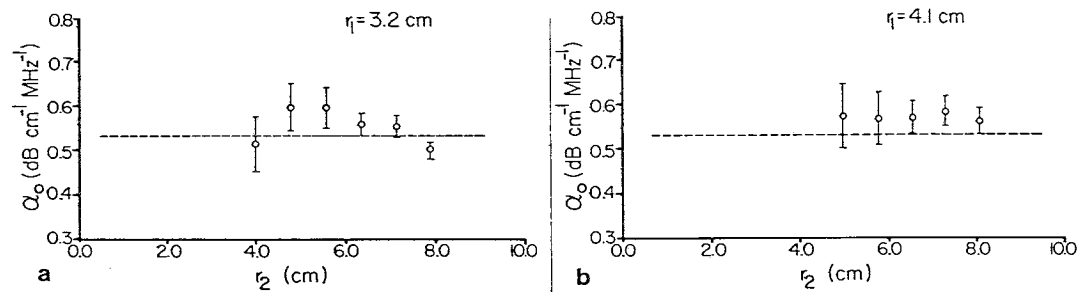

Fig. 9 Measurements of α_o for TM nonfat A through a constant thickness layer (2 cm) of TM fat material (phantom II, surface 4). A 3.5 MHz/13 mm transducer was used in (a) and a 3.5 MHz/19 mm transducer was used in (b). Corrections which account for the transducer beam were used. The dotted line marks the known α_o value of 0.53 dB cm-1 MHz-1.

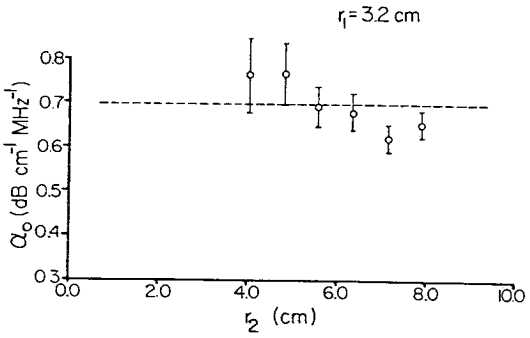

Fig. 10 Measurements of α_o using the spectral difference method for phantom III, scanning surface 6. The TM material in phantom III is composed of a combination of intermediate and small particle scatterers. Mean power spectra measured at various C-plane depths, r_2, were compared with the spectrum measured at 3.2 cm (r_1). Corrections for the transducer beam were used in the analysis. The dashed line marks the known α_o value of 0.70 dB cm^{-1} MHz^{-1}.

V. ERROR ANALYSIS

The uncertainty in attenuation measured using the spectral difference technique is calculated using a method described by Bevington [17]. The errors are propagated from uncertainties in independent variables used to determine values of α_o using the relation

$$\Delta\alpha_o = \left[\sum_{i=1}^{5} \left(\frac{\partial \alpha_o}{\partial x_i} \right)^2 \Delta x_i^2 \right]^{1/2} \tag{9}$$

Those variables are $S(r_1,f)$, $S(r_2,f)$, $X(r_1,f)$, $X(r_2,f)$, and Δr.

A number of factors contribute to the uncertainty in the measured power spectra. The specifications for the waveform digitizer quote an attenuator accuracy of ± 3 percent, a resolution of $\pm$ 0.4 percent (1/256), and the gain stability at $\pm$ 1 percent over 4 hrs. (Gould Inc., Santa Clara, CA). The effective apperture uncertainty of the digitizer is quoted by the manufacturer as being less than 2 ns. The above factors contribute very little to the overall uncertainty. The precision of the measurement, shown by the error bars in figures 7 through 10, is, however, the dominant factor in determining the uncertainty in measured power spectra. (The error bars denote one standard deviation of the mean.) This variability is primarily due to the stochastic nature of the scattering medium and varies with the separation between measurement planes, Δr, and number of spectra averaged, M. We found that by averaging the spectra from twenty-five uncorrelated waveform segments, the magnitude of the observed error varied between 16 percent of the measured value for a separation of 0.8 cm and 4 percent for a 6.1 cm separation.

A one percent error in the phantom depth is possible considering the uncertainty in the speed of sound and the delay time measurements. This value will increase for <u>in vivo</u> measurements, where the speed of sound varies to a greater extent.

Combining all of the above uncertainties using Eq. (9), the total uncertainty in α_o for a typical measured value of 0.55 dB cm^{-1} MHz^{-1} is $\pm$ 0.17 dB cm^{-1} MHz^{-1} for Δr = 0.8 cm and $\pm$ 0.04 dB cm^{-1} MHz^{-1} for Δr = 6.1 cm. Both the precision and the accuracy of the measurement improves as

the amount of attenuating material between the measurement depths increases.

VI. DISCUSSION

The results of figures 7 and 10 show that for homogeneous materials, the spectral difference method yields measurements of α_o that agree with narrow-band substitution measurements. Such results were obtained independent of the choice of depths r_1 and r_2 in the medium. This independence is a result of accounting for the transducer beam diffraction pattern. A transducer's size, focusing, and bandpass characteristics all determine the correction factors, X(r,f), used in Eq. (8).

When diffraction effects are not included in the data analysis, attenuation estimates using the spectral difference method vary depending on the position of the C-planes. Disagreements with the substitution measurements were as large as 40 percent.

Ophir et al. [4] has measured attenuation coefficients, in vivo, using a method which avoids effects due to the beam pattern. In their C-scan technique, measurements at two depths in tissue are made, each at the focal length of the transducer. This is accomplished by positioning the transducer at two distances from the skin surface using a water stand-off. However, not being able to maintain skin contact may offer some clinical disadvantages. During a liver scan, for example, it is often necessary to press the transducer onto the skin surface to gain access to tissues which lie beneath the ribs. The spectral difference method described in this report could permit attenuation measurements to be obtained along with present diagnostic procedures.

The results of the phantom simulations suggest that a significant effect on in vivo attenuation measurements is possible when inhomogeneous tissues are interposed between the transducer and the scattering volume. Measurements of α_o for most conditions in which either of the two irregular TM fat layers intervened (Fig. 8) were greater than the value expected. Under such conditions, phase cancellation across the transducer surface and beam refraction could both contribute to this measurement error [10,11]. The results of figures 8a and 8b show that as the separation between the C-planes (Δr) increases, the corresponding measurements of α_o approach the expected value. Thus, it is the greater attenuation accompanying large C-plane separations which becomes the dominant cause of variation between the spectra measured at the two depths. The effect of the irregular TM fat layers on measurements of α_o also seem to be lessened when using the larger aperture, 19 mm transducer (compare figures 8b and 8c). Therefore, the proper choice of transducer size and C-plane depth can increase the accuracy of in vivo attenuation measurements, even in the presence of distortions from intervening, inhomogeneous tissues. Since the measurements from spectra obtained through a planar TM fat layer (Fig. 9), for both transducers, were very close to the values expected, the perturbing effects seen in figure 8 are due to the irregularity of the TM fat-nonfat interface and not simply due to the presence of the inhomogeneous layer.

VII. SUMMARY AND CONCLUSIONS

Modifications to the spectral difference method originally proposed by Kuc [2,3] have yielded attenuation measurements which closely agree

[8] Goss, S.A., Johnston, R.L., and Dunn, F., Comprehensive compilation of empirical ultrasonic properties of mammalian tissues, J. Acoust. Soc. Am. 64, 423-457 (1978).

[9] Hottier, F., Fink, M. and Berger, G. Experimental estimation of ultrasonic attenuation in liver using short-time Fourier analysis: influence of system parameters, Ultrasonic Imaging 4, 178 (1982), abstract only.

[10] O'Donnell, M., Phase Insensitive Pulse-Echo Imaging, Ultrasonic Imaging 4, 321-335 (1982).

[11] Shung, K.K. and Dzierzanowski, J.M., Effects of phase-cancellation on scattering measurements, Ultrasonic Imaging 4, 56-70 (1982).

[12] Madsen, E.L., Zagzebski, J.A., and Frank, G.R., Oil-in-gelatin dispersions for use as ultrasonically tissue-mimicking materials, Ultrasound Med. Biol. 8, 277-287 (1982).

[13] Madsen, E.L., Zagzebski, J.A., Banjavic, R.A., and Jutila, R.E., Tissue-mimicking materials for ultrasonic phantoms, Med. Phys. 5, 391-394 (1978).

[14] Insana, M.F., Zagzebski, J.A., and Madsen, E.L., Acoustic backscattering from ultrasonically tissue-like media, Med. Phys. 9, 848-855 (1982).

[15] Madsen, E.L., Zagzebski, J.A., and Frank, G.R., A dynamic perfusion phantom for use in ultrasonically induced hyperthermia, International J. Radiation Oncology, Biol. Phys., in press (1983).

[16] Madsen, E.L., Zagzebski, J.A., Insana, M.F., Burke, T.M., and Frank, G.R., Ultrasonically tissue-mimicking liver including the frequency dependence of backscatter, Med. Phys. 9, 703-710 (1982).

[17] Bevington, P.R., Data Reduction and Error Analysis for the Physical Sciences (McGraw-Hill, New York, 1969).

[18] Gonzalez, R.C., Wintz, P., Digital Image Processing Applied Mathematics and Computation Series No. 13, pp. 41-88 (Addison-Wesley, Massachusetts, 1977).

[19] Kuc, R., Modeling and estimating reflected signal spectra, Ultrasonic Imaging 4, 177 (1982), abstract only.

[20] O'Donnell, M., Effects of diffraction on measurements of the frequency-dependent ultrasonic attenuation, IEEE Trans. Biomed. Engineering, BME-30, 320-326 (1983).